IJMMM International Journal of Minerals, Metallurgy and Materials 矿物冶金与材料学报（英文版）

Effect of titanium content on the refinement of coarse columnar austenite grains during the solidification of peritectic steel

Jiazhi An, Zhaozhen Cai, and Miaoyong Zhu

Cite this article as:
Jiazhi An, Zhaozhen Cai, and Miaoyong Zhu, Effect of titanium content on the refinement of coarse columnar austenite grains during the solidification of peritectic steel, *Int. J. Miner. Metall. Mater.*, 29(2022), No. 12, pp. 2172-2180. https://doi.org/10.1007/s12613-021-2375-2

International Journal of Minerals, Metallurgy and Materials
Volume 29, Number 12, December 2022, Page 2172
https://doi.org/10.1007/s12613-021-2375-2

Effect of titanium content on the refinement of coarse columnar austenite grains during the solidification of peritectic steel

Jiazhi An[1,2], *Zhaozhen Cai*[1,2)✉], *and Miaoyong Zhu*[1,2)✉]

1) Key Laboratory for Ecological Metallurgy of Multimetallic Mineral (Ministry of Education), Northeastern University, Shenyang 110819, China
2) School of Metallurgy, Northeastern University, Shenyang 110819, China
(Received: 18 July 2021; revised: 3 November 2021; accepted: 8 November 2021)

Abstract: The effect of titanium content on the refinement of austenite grain size in as-cast peritectic carbon steel was investigated by fast directional solidification experiments with simulating the solidification and growth of surface and subsurface austenite in continuously cast slabs. Transmission electron microscope (TEM) and scanning electron microscope (SEM) were used to analyze the size and distribution of Ti(C,N) precipitates during solidification. Based on these results, the pinning pressure of Ti(C,N) precipitates on the growth of coarse columnar grains (CCGs) was studied. The results show that the austenite microstructure of as-cast peritectic carbon steel is mainly composed of the regions of CCGs and fine columnar grains (FCGs). Increasing the content of titanium reduces the region and the short axis of the CCGs. When the content of titanium is 0.09wt%, there is no CCG region. Dispersed microscale particles will firstly form in the liquid, which will decrease the transition temperature from FCGs to CCGs. The chain-like nanoscale Ti(C,N) will precipitate with the decrease of the transition temperature. Furthermore, calculations shows that the refinement of the CCGs is caused by the pinning effect of Ti(C,N) precipitates.

Keywords: peritectic steel; grain refinement; coarse columnar grain; titanium carbonitride; pinning pressure

1. Introduction

Peritectic steel is one of the main products of steel manufacturers and is widely used in the automobile manufacturing, shipbuilding, construction of bridges, pipelines and offshore platforms, etc. However, during continuous casting of peritectic steel, the solidifying shell is susceptible to cracking, which generally results from the presence of coarse columnar γ grains (CCGs) [1]. In general, surface cracks form along the CCGs from the slab surface to the interior and steel manufacturers need to perform offline cleaning [2–3]. Whether the prevention of the formation of CCGs can control the surface cracks on peritectic steel slabs, is a significant question.

During the solidification of peritectic steel, the primary ferrite phase grows along the temperature gradient and forms columns. When the temperature drops to the peritectic reaction temperature (T_P), γ-phase begins to form at the boundary of the δ-phase through the peritectic reaction, $L + \delta \rightarrow \gamma$. In this stage, γ-phase is composed of fine columnar grains (FCGs), and the length of the short axis of the γ-phase is a good approximation to the primary dendrite arm space, which results from the pinning of the remaining liquid or δ-phase. When the temperature decreases to the temperature of austenite completion transformation (T_γ), the temperature at which the austenite transformation is completed, the pinning phase disappears, and the fine columnar austenite grains begin to grow by a massive transformation into coarse columnar grains [4–5]. Many works have studied the mechanisms for the formation and transformation of FCGs. Some studies indicated that FCGs grow continuously and eventually convert to CCGs when the temperature falls below T_γ, as shown in Fig. 1(a) [6–8]. Recent studies using solidification equipment and phase-field simulations suggested that the transformation from FCGs to CCGs is discontinuous, and the formation of CCGs is accompanied by the rapid movement of FCG/CCG region boundaries (FCRB) along the unidirectional temperature gradient, as shown in Fig. 1(b) [9–10].

Ferrite stabilizing elements such as phosphorus, aluminum, or chromium could refine the CCGs by decreasing T_γ to retard the motion of the FCRB by the discontinuous growth mechanism [11–13]. In addition to stabilize the liquid or δ phase at a lower temperature, the carbonitride particles formed by adding microalloying elements, such as titanium, can effectively refine the austenite grain size. Many studies have shown that fine titanium carbide, nitride, and carbonitride particles can effectively retard γ-grain growth; however, most of these studies focused on the influence of titanium carbonitrides on the growth of austenite grains in the single-phase austenite region and the inhibition of austenite grain boundary movement at a single cooling rate [14–19]. Ohno and Matsuura [20] studied the refinement of austenite microstructure of S45C steel during the solidification process by titanium addition, but the formation of austenite grains in

✉ Corresponding authors: Zhaozhen Cai E-mail: caizz@smm.neu.edu.cn; Miaoyong Zhu E-mail: myzhu@mail.neu.edu.cn

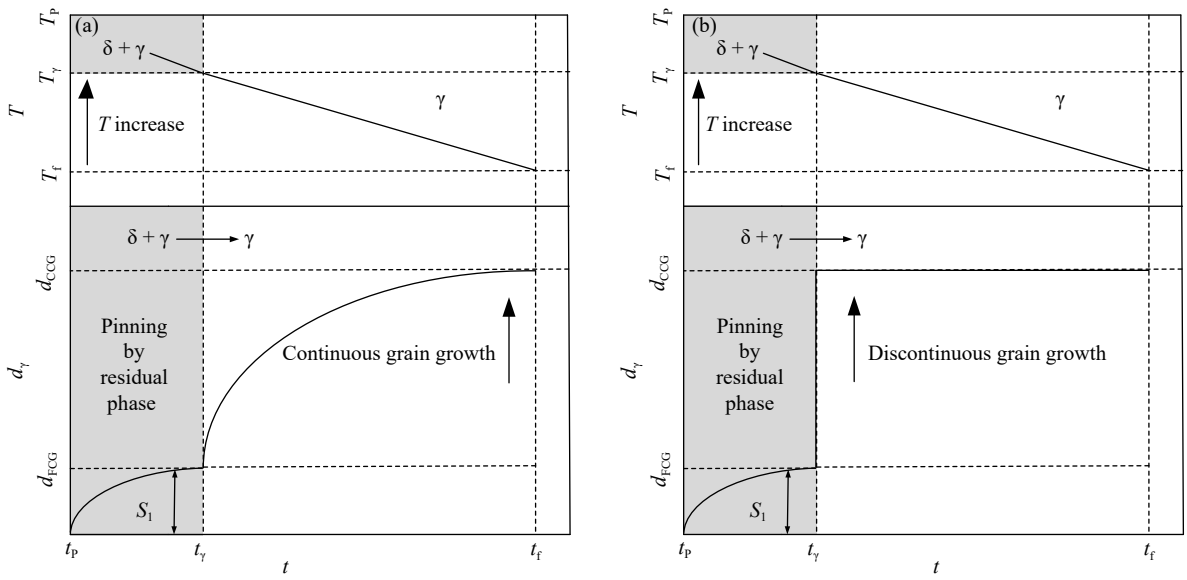

Fig. 1. Schematic of the austenite grain growth: (a) continuous grain growth [8], (b) discontinuous grain growth. T represents temperature; T_f is the finish temperature of γ growth; d_γ is the short-axis diameter of γ grains; d_{FCG} and d_{CCG} are the short-axis diameter of FCGand CCG, respectively; t represents time; t_p is the peritectic reaction time; t_γ is the time of austenite completion transformation; t_f is the finish time of γ growth; S_1 is the primary dendrite arm space.

S45C steel originates from the primary solidification of the γ phase rather than discontinuous growth [21]. The suppressive effect of titanium on the formation of CCGs during the solidification of peritectic steel has not been investigated in terms of the discontinuous growth mechanism.

Considering that CCGs tend to form during the continuous casting process of peritectic carbon steels with 0.15wt% carbon [1,22], the present work investigates the solidification of this type of steel by fast directional solidification equipment. The morphologies and sizes of Ti(C,N) particles are studied by Transmission electron microscope (TEM) and scanning electron microscope (SEM). The influence of titanium content on the suppression of the formation and growth of CCGs is quantitatively investigated during the solidification process of peritectic steel.

2. Experimental

The present work studied the solidification of peritectic steel with 0.15wt% C; Fe–28.5wt%Ti alloy was melted to fabricate the steel samples with titanium contents from 0.01wt% to 0.09wt%. These steels were referred to as 0.01Ti, 0.03Ti, 0.06Ti, and 0.09Ti samples in this paper, and their detailed composition is shown in Table 1. The solidification of these samples was carried out by a fast-directional solidification experiments, as shown in Fig. 2. The device includes a cooled copper mold and a corundum tube. The water-cooling copper plate represents the mold in practical continuous casting. The cooling rate can be controlled by adjusting the water flow. During the experiment, molten steel was poured into the preheated corundum tube to simulate directional solidification.

The detailed experimental process is as follows. The 0.15wt% C steel and Fe–28.5wt%Ti alloy, approximately 350 g total, were put into an alumina crucible and melted at 1570°C in a tube furnace filled with argon gas (>99.999%). The inner diameter and depth of the alumina crucible were 40 mm and 70 mm, respectively. After holding for 1 h at 1570°C, the melt was cast into the fast directional solidification experiments, where the corundum tubes were preheated at 1570°C. The molten steel solidified unidirectionally from the bottom to the top. A sample with a height of 55 mm and diameter of 32 mm was quenched in cold water to obtain a proeutectoid ferrite film when the surface temperature dropped to approximately 900°C.

The columnar sample was sliced vertically through its center axis. A rectangular area at the center was etched by 4vol% nital and inspected by optical microscopy (OM). The observation region was focused from the bottom to a height of 25 mm. Titanium precipitates were mainly divided into two types: microscale particles (diameter approximately 1 to 10 μm) [23], and nanoscale precipitates (diameter approximately 5 to 300 nm) [24]. The morphology and composition of the microscale particles were detected by an ULTRA PLUS field emission scanning electron microscope (FESEM) with energy-dispersive spectrometry (EDS). A G20 TEM with

Table 1. Chemical composition of the experimental steels wt%

Sample	C	Si	Mn	P	S	N	Ti	Fe
0.01Ti	0.15	0.175	0.41	0.025	0.028	0.005	0.011	Bal.
0.03Ti	0.151	0.176	0.42	0.026	0.027	0.0054	0.028	Bal.
0.06Ti	0.149	0.172	0.41	0.025	0.027	0.0052	0.063	Bal.
0.09Ti	0.152	0.176	0.43	0.024	0.029	0.0055	0.087	Bal.

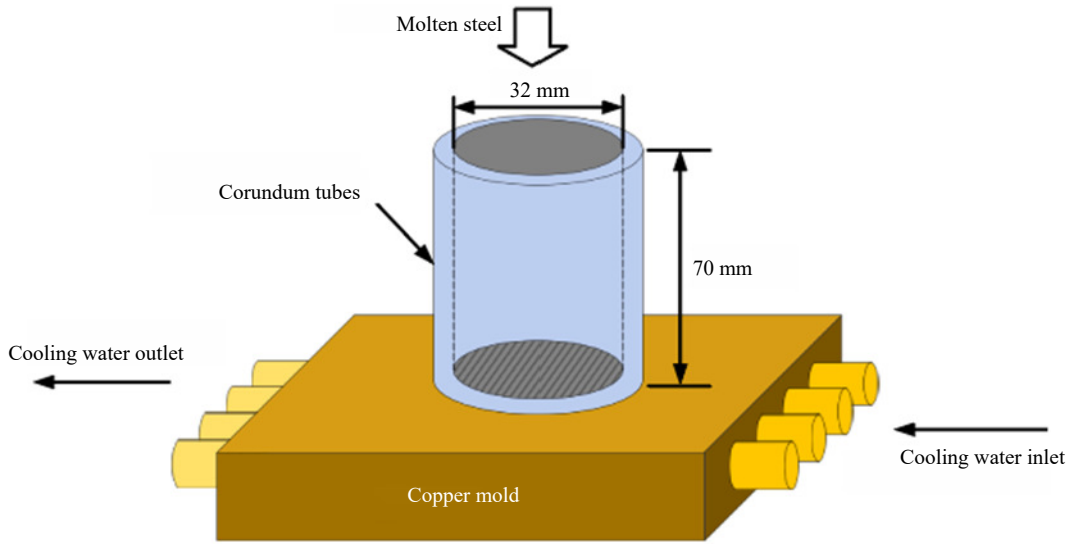

Fig. 2. Schematic illustration of fast cooling equipment device.

EDS was also used to observe the size and distribution of the nanoscale precipitates, and the preparation of TEM specimens was described below: the specimens were cut to 500 μm by wire cutting, and they were polished down to 50–60 μm by using the sandpaper. Afterward, they were thinned through twin-jet electropolishing device in 5vol% perchloric acid ethanol solution.

3. Results and discussion

3.1. Microstructures of the as-cast γ grain

Fig. 3(a_1)–(d_1) shows the as-cast γ grain structures in the samples with titanium contents varying from 0.01wt% to 0.09wt%. The CCG boundaries traced from the macrograph are shown at the bottom of each macrograph, as shown in

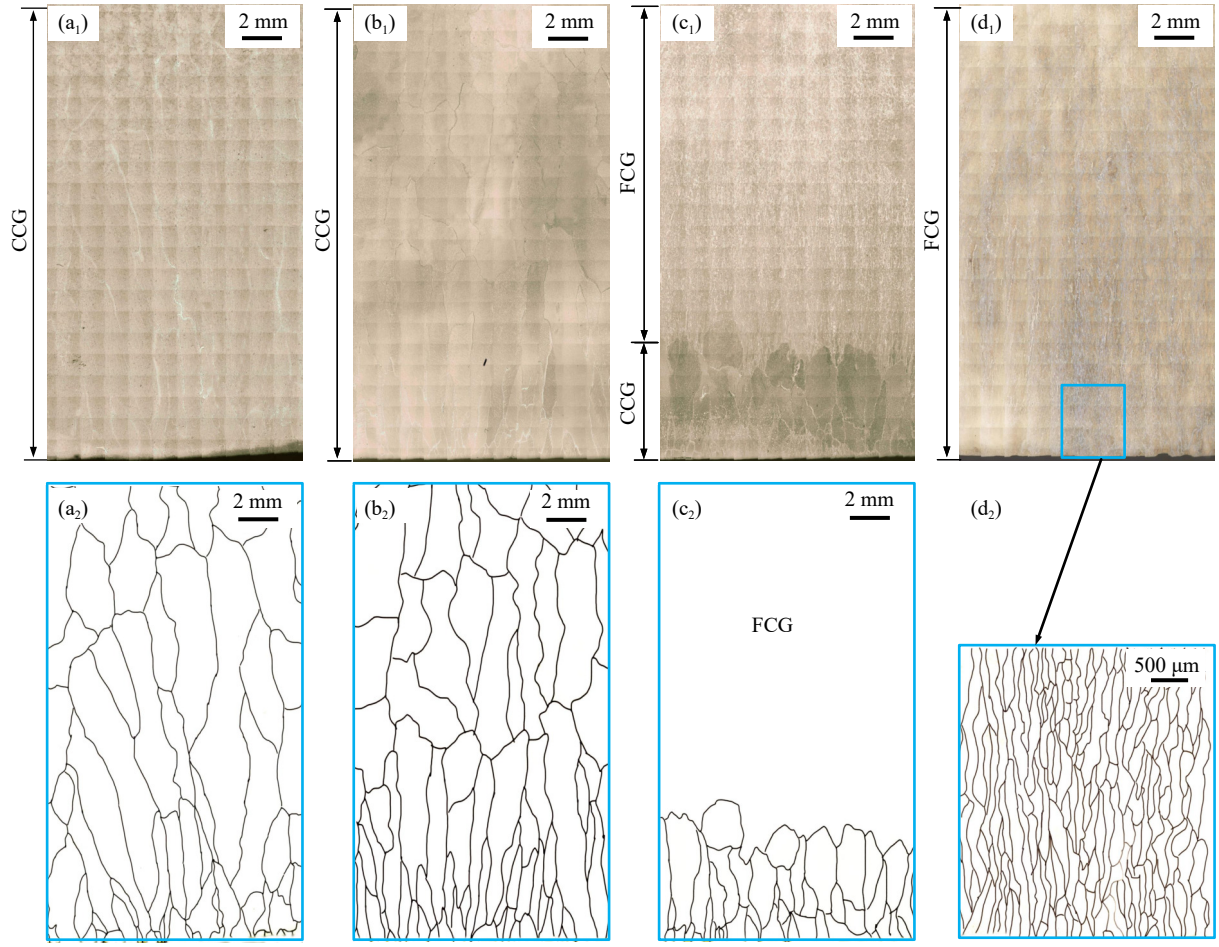

Fig. 3. Microstructures of (a_1) 0.01Ti, (b_1) 0.03Ti, (c_1) 0.06Ti, and (d_1) 0.09Ti samples. The CCG boundaries traced of the samples with (a_2) 0.01Ti, (b_2) 0.03Ti, (c_2) 0.06Ti, and (d_2) 0.09Ti samples. The bottom of each macrograph corresponds to the surface of the sample.

Fig. 3(a_2)–(d_2). The bottom of the micrograph corresponds to the surface of the sample, and the top corresponds to the center of the sample. In the 0.01Ti and 0.03Ti samples, the GGGs develop from the surface toward the center of the sample along the direction of heat flow, which have a short-axis diameter with a few mm. When the titanium content is 0.06wt%, the austenite structure is significantly different, as shown in Fig. 3(c_1). CCGs still form and grow from the surface to the center of the sample, but none are present 7.2 mm from the surface. The addition of 0.06wt% titanium suppresses the growth of CCGs. The further addition of titanium leads to the absence of the CCG region, and the structure only consists of FCGs, as shown in Fig. 3(d_2), which is the enlargement of the FCG structure at the surface of samples in Fig. 3(d_1).

The short-axis diameter of CCG and FCG is obtained by the intercept method and the schematic for the measurement of the short-axis diameter of CCG and FCG is shown in Fig. 4. L_1 and L_2 represent the measure length of CCG and FCG, respectively. N_1 is the number of CCG in L_1, and N_2 is the number of FCG in L_2. Fig. 5 shows the relationship between the γ grain size and titanium content. In particular, the short-axis diameters of the γ grains of 0.153wt%C–0.2wt%Si–0.025wt%P–0.03wt%S steel in continuously cast slabs are represented in Fig. 5 (as shown in the black line of the figure). The γ structure in the practical continuous casting (CC) is shown in Fig. 6. The bottom of each image corresponds to the surface of the slab. The structure and sizes of γ grains in continuous cast slabs are very similar to that of the 0.01wt% titanium sample, as determined by comparing Fig. 6 and Fig. 3(a_1), which indicates that the current experimental conditions are quite similar to those of practical continuous casting. In the 0.01Ti and 0.03Ti samples, the short-axis diameters of the CCGs gradually increase with increasing distance from the surface due to the decrease in cooling rate. The short-axis diameters of the γ grains drastically decrease

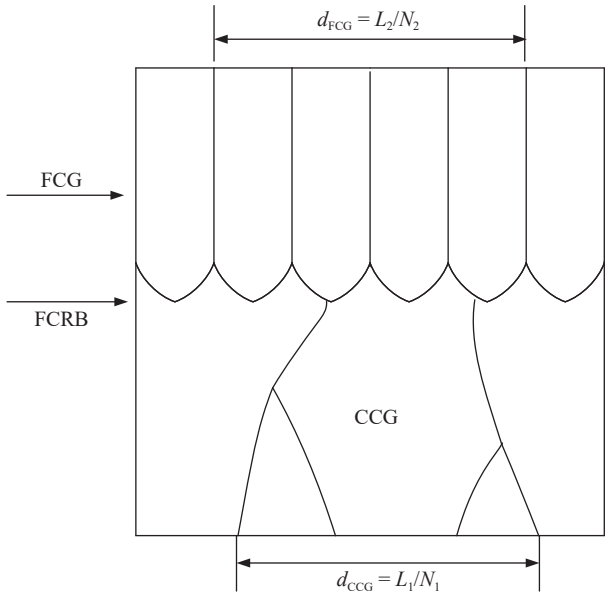

Fig. 4. Schematic of the short-axis diameter of FCG and CCG.

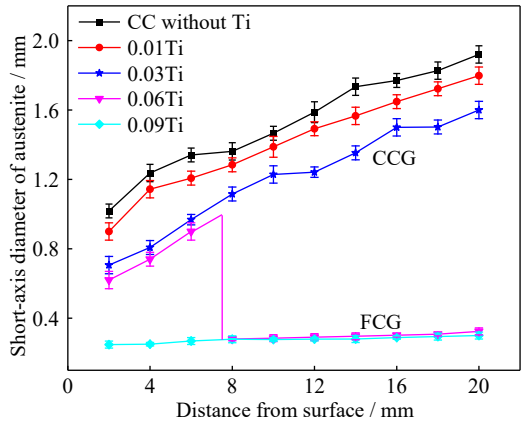

Fig. 5. Relationship between the short axis diameter of austenite and the distance from the surface of the sample.

from a few millimeters to 200–300 μm at 7.2 mm from the surface, which shows that the discontinuous grain growth of the CCGs is prevented and FCGs remain in the 0.06Ti sample. Furthermore, the short axis-diameter of the γ grains is approximately 200–300 μm in the 0.09Ti sample, which indicates that the growth of the CCGs is suppressed completely. The short-axis diameter of the CCGs decreases with increasing titanium content, as shown in Fig. 5. The above analysis shows that the addition of titanium not only decreases the short-axis diameter of the CCGs but also suppresses the growth of the CCGs.

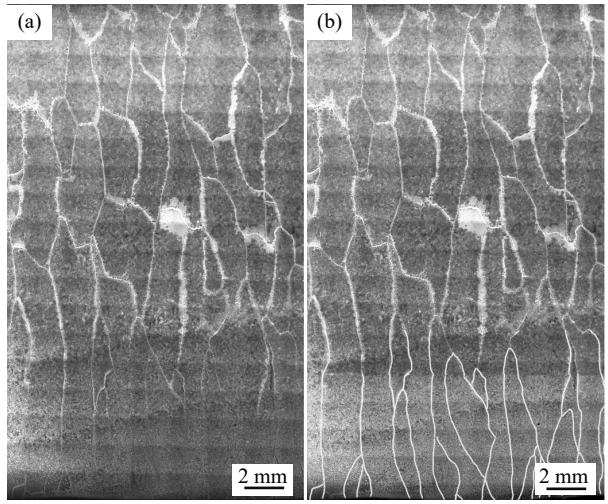

Fig. 6. Micrographs of practical continuously cast slabs: (a) the as-cast γ structure; (b) the trace of γ structure.

3.2. Morphology and size distribution of Ti(C,N) particles

CCG growth in the solidification process of peritectic steel is discontinuous accompanied by FCRB movement. Without considering the inhibitory effect of adding titanium on the discontinuous growth of CCGs, the temperature at the FCRB is always equal to T_γ [10–11]. When the temperature drops below T_γ, the FCGs rapidly grow into CCGs accompanied by the disappearance of the δ phase. Therefore, the refinement of CCGs can be achieved by the following two methods: one is to decrease the T_γ, thereby decreasing the activation energy

during the transition from FCGs to CCGs; the other is to introduce a new pinning phase to suppress FCRB movement after the δ phase disappears. In this study, the addition of titanium not only suppresses the movement of the FCRB but also reduces the short-axis diameter of the CCGs. To investigate the influence of titanium on the refinement of CCGs, the phase diagram of the Fe–0.15wt%C–0.41wt%Mn–0.025wt%P–0.175wt%Si–0.028wt%S–0.05wt%N–*x*Ti quaternary system was analyzed by Factsage 7.3 thermodynamic software, as shown in Fig. 7. The T_γ values of 0.01Ti, 0.03Ti, 0.06Ti, and 0.09Ti steels are 1489.15, 1485.31, 1484.54, and 1483.16°C, respectively. The difference in T_γ values is not significant, which indicates that the change in T_γ by adding titanium can be ignored. However, when the titanium content is 0.012wt%, Ti(C,N) begins to precipitate before the temperature drops to T_γ, and this is likely to be the new pinning phase that retard the growth of CCGs after the δ phase disappears.

As shown in Fig. 3, when the titanium content is 0.06wt%, the CCGs disappear and the FCG is retained at a position approximately 7.2 mm from the surface, which means that discontinuous growth is suppressed. Therefore, this paper takes the position of 7.2 mm from the surface as the research object. The formation of CCGs only occurs at the moment when the pinning phase disappears, and the size of CCGs remains unchanged in the subsequent solidification process, according to the discontinuous growth mechanism. After the FCRB moves to 7.2 mm below the surface, the growth of Ti(C,N) has no significant influence on the final microstructure of austenite. Therefore, the present work focuses on the transient pinning effect of particles containing Ti(C,N) when the FCRB moves 7.2 mm from the surface.

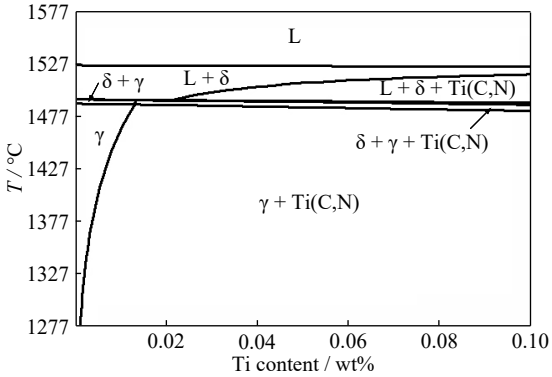

Fig. 7. Phase diagram of Fe–0.15wt%C–0.41wt%Mn–0.025wt%P–0.175wt%Si–0.028wt%S–0.05wt%N–*x*Ti calculated by FactSage software.

In order to investigate the transient pinning effect of Ti(C,N) particles on the FCRB, the samples were quenched in an ice water bath after different solidification times. The results show that it takes approximately 30 s for the FCRB to move from the surface to approximately 7.2 mm at the same experimental condition in the 0.06Ti sample, as shown in Fig. 8. Furthermore, the average height of CCG region at solidification of 30 s decreases with the increase of titanium content, which means that the transition temperature from FCG to CCG decreases.

In addition to check the cooling condition at 7.2 mm away from the surface, the cooling curve was measured by setting Platinum and Rhodium thermocouple inside the sample. Fig. 9 shows the temperature changes for 0.06Ti sample. The T_γ in different samples calculated by Factsage 7.3 thermodynamic software and the temperature at 7.2 mm ($T_{7.2\,mm}$) after solidification of 30 s are also presented in the Fig. 9. As can be seen from the figure, the temperature at 7.2 mm after solidification of 30 s was 1359.10°C. The precipitate of Ti(C,N) can be divided into two categories when the titanium content was above 0.03wt%: one was microscale Ti(C,N) precipitating in the liquid or/and δ phase when the temperature varied from the 1570°C to T_γ and the other was nanoscale Ti(C,N) precipitating in the γ phase when the temperature varied from the T_γ to 1359.10°C. Based on the above analysis, the inhibitory effect of Ti(C,N), including microscale particles and nanoscale precipitates, on the discontinuous growth of CCG was quantitatively studied by investigating the size and distribution of Ti(C,N) at the height of 7.2 mm distance from the surface.

The nanoscale precipitates with different titanium contents observed at approximately 7.2 mm from the surface are illustrated in Fig. 10. Through the analysis of the typical pre-

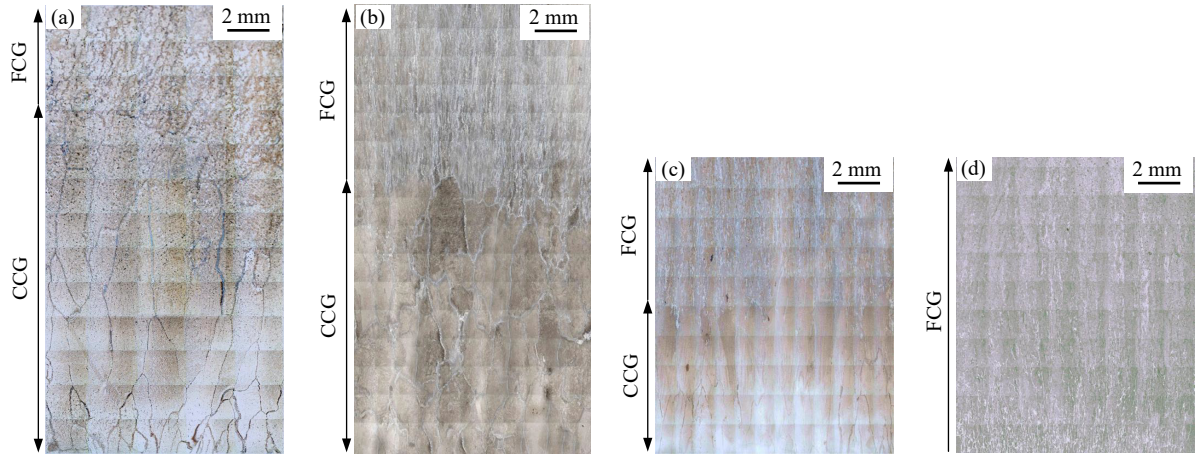

Fig. 8. Micrographs of the γ structure quenched for 30 s: (a) 0.01Ti, (b) 0.03Ti, (c) 0.06Ti, and (d) 0.09Ti. The bottom of the micrograph corresponds to the surface of the sample.

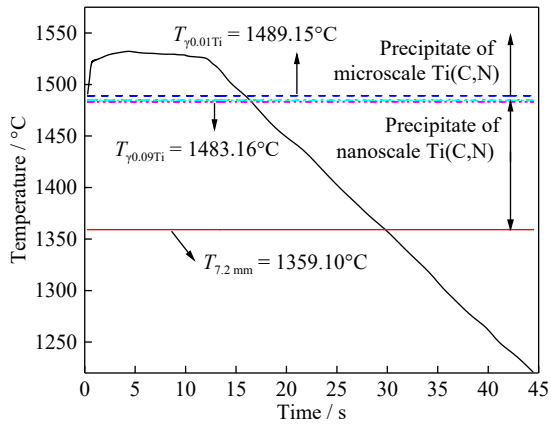

Fig. 9. Temperature change curves at 7.2 mm away from the surface.

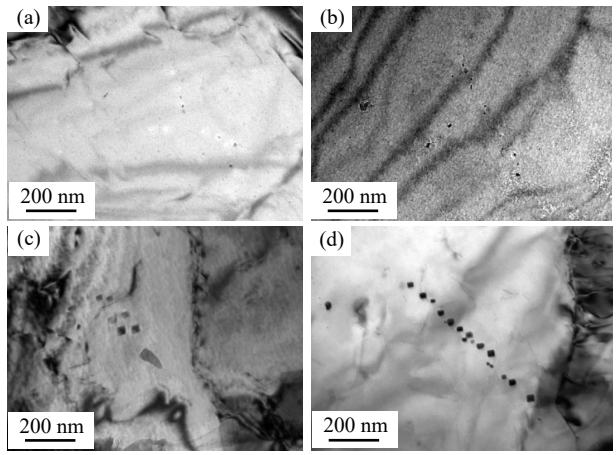

Fig. 10. Morphology of nanoscale precipitates in different samples: (a) 0.01Ti, (b) 0.03Ti, (c) 0.06Ti, and (d) 0.09Ti.

cipitate in 0.06Ti sample by EDS, the quadrates precipitations are identified as Ti(C,N), as shown in the Fig. 11. A few scattered precipitates were distributed in the matrix when the titanium content was 0.01wt%. Furthermore, the size and quantity of precipitates increased dramatically with increasing titanium content. Carbonitride precipitates were arranged in chain-like conformations, and chain-like precipitates were distributed on γ grain boundaries [25], which reduced the short-axis diameter in austenite. However, the effect of chain-like Ti(C,N) particles on discontinuous growth, especially the suppressive effect on the migration of the FCG/CCG boundary, has not been reported and will be discussed further below.

The morphology and size distribution of microscale Ti(C,N) particles at the central position of the 7.2 mm distance from the surface after solidification of 30 s and EDS analysis are shown in Fig. 12. Microscale particles are not found in the steel with titanium contents below 0.03wt%. The particles containing Ti(C,N) are indicated by EDS, as illustrated in Fig. 12(e) and (f). When the Ti concentration reached 0.06wt%, Ti(C,N) particles began to precipitate, as shown in Fig. 12(a). With the titanium content was 0.09wt%, the number of Ti(C,N) particles increased sharply, while there was no significant change in particle size. Ti(C,N) particles were uniformly distributed without a chain-like conformation. The effect of microscale Ti(C,N) particles on discontinuous growth, especially in inhibiting the migration of the FCG/CCG boundary, has not yet been reported yet, which will also be discussed further below with nanoscale Ti(C,N) precipitates.

3.3. Influence of Ti(C,N) on the discontinuous growth of CCGs

The growth of CCGs is accompanied by movement of the FCRB, according to the discontinuous grain growth theory, and the migration rate of FCRB, V_γ, during the CCG formation process is written as [10]:

$$V_\gamma = m\left(T_\gamma\right)\frac{\sigma}{\varepsilon d_{FCG}} \tag{1}$$

where d_{FCG} is the short-axis diameter of the FCGs, ε is a constant determined by the local shape of the FCRB, which is approximated to 0.78 [10], $m(T_\gamma)$ represents the kinetic constant for the grain boundary mobility, σ is the grain boundary interfacial energy and is set to be 0.79 J·m^{-2} [26]. From Eq. (1), the migration velocity of the FCG/CCG boundary is inversely proportional to the short-axis diameter of the FCGs.

The pinning pressure, P_p, exerting on the FCRB, which is

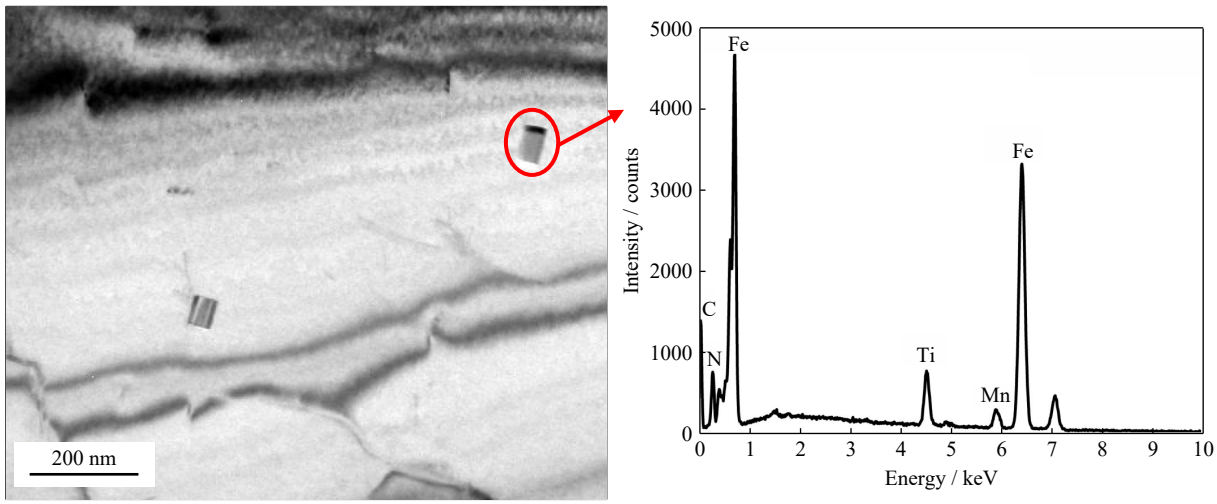

Fig. 11. Composition identification of the precipitates by EDS.

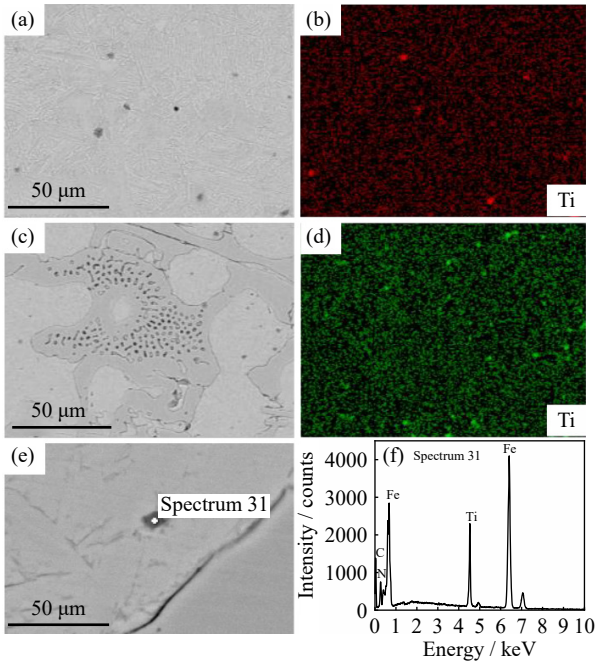

Fig. 12. Morphology and size distribution of microscale Ti(C,N) particles and EDS analysis of different samples: (a) 0.06Ti; (b) elemental distribution from EDS analysis of (a); (c) 0.09Ti; (d) elemental distribution by EDS analysis of (b); (e, f) composition of precipitates by EDS.

due to the presence of Ti(C,N) particles, is written as [26]:

$$P_{\mathrm{p}} = k\frac{\sigma f}{r} \tag{2}$$

where f represents the volume fraction of the Ti(C,N) particles, r is the mean radius of Ti(C,N) particles, and k is a constant and considered to be 1.33 [26].

When Ti(C,N) particles exist, V_γ can be expressed in the following form by bringing the Eq. (2) into the Eq. (1),

$$V_\gamma = m\left(T_\gamma\right)\left(\frac{\sigma}{\varepsilon d_{\mathrm{FCG}}} - k\frac{\sigma f}{r}\right) \tag{3}$$

which can be expressed as:

$$V_\gamma = m\left(T_\gamma\right)\left(P_{\mathrm{d}} - P_{\mathrm{p}}\right) \tag{4}$$

where P_{d} is driving pressure exerted on the FCG/CCG region boundary.

When P_{p} is greater than P_{d}, the migration velocity of the FCG/CCG boundary is completely suppressed, and CCGs do not form according to Eq. (2). Importantly, the P_{d} is determined by the volume fraction and the mean radius of the Ti(C,N) particles, which consists of two parts: the pinning pressure provided by microscale Ti(C,N) particles, P_{pm}, and the pinning pressure provided by nanoscale Ti(C,N) precipitates, P_{pn}.

The volume fraction was obtained by the method of MaCall-Boyd [27], which was required to measure the diameter of each Ti(C,N) particle in certain areas from the SEM or TEM image, calculating the number of Ti(C,N) particles, and finally converting the data into the average diameter. The volume fraction was acquired by the MaCall-Boyd method according to the following equation:

$$f = \left(\frac{\pi}{3}\right)\cdot\left[\frac{Nd^3}{Ad_{\max}}\right] \tag{5}$$

where N is the number of Ti(C,N) particles, A represents the area of the measured field, $d_{\max}$ is the maximum diameter, and d is the mean diameter in the measured field.

Fig. 13 demonstrates the variation in the size and volume fraction of Ti(C,N) particles with different titanium contents. The size and volume fraction of nanoscale precipitates increase with titanium addition. The average size of the precipitates increases from 2.4 nm in the 0.01Ti sample to 30.2 nm in the 0.09Ti sample. The volume fraction of precipitates dramatically increases from 0.0007% to 0.023% accompanied by an increase in the amount and size of Ti(C,N) precipitates. The size of the microscale particles falls slightly to approximately 2.64 μm in the 0.09Ti sample from 2.98 μm in the 0.06Ti sample. Even so, the volume fraction still drastically increases. This is principally because the number of Ti(C,N) particles in the 0.09Ti sample is far greater than that in the 0.06Ti sample. This behavior is also reflected in Fig. 12.

Fig. 14 shows the driving pressure required for the formation of CCGs, P_{d}, and the pinning pressure provided by Ti(C,N) particles with different titanium contents. The figure shows that the influence of Ti(C,N) particles on the growth of CCGs mainly includes two aspects: the P_{d} slightly increases, and the pinning pressure substantially increases, with in-

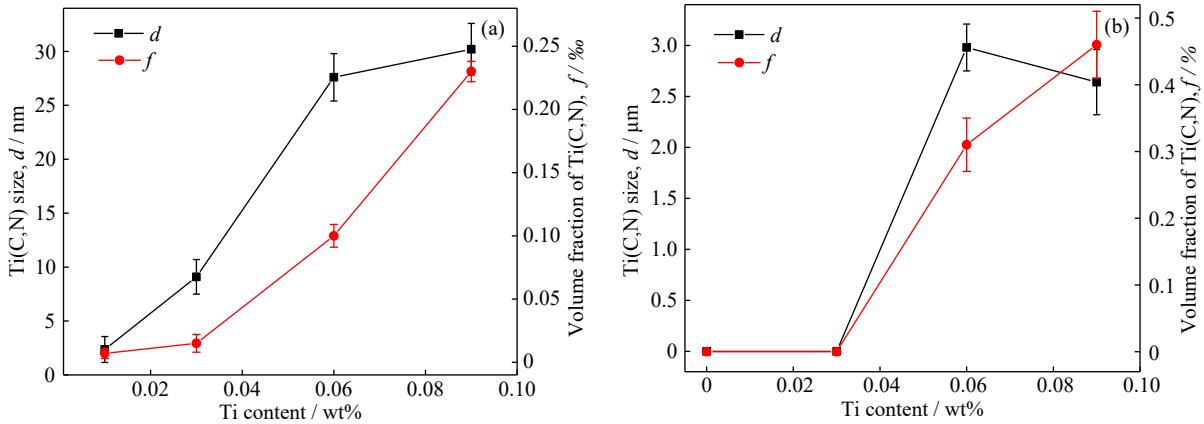

Fig. 13. Size and volume fraction of Ti(C,N) particles in samples with different titanium contents under different scale: (a) nanoscale; (b) micronscale.

creasing Ti content, especially the P_{pn}. When the titanium content was 0.01wt% or 0.03wt%, the driving pressure was greater than the pinning pressure, and discontinuous growth continued to occur at this position. When the content of titanium increased to 0.06wt%, the pinning pressure provided by microscale and nanoscale Ti(C,N) was 7.75 kJ·m^{-3}, which was greater than the driving pressure with the value of 4.75 kJ·m^{-3} at 7.2 mm distance from the surface, and the discontinuous growth was suppressed. The pinning pressure was far great than the driving pressure with the further addition of titanium. It should be pointed out that P_{pm} was far less than P_{pn}. In other words, the inhibition of CCGs in the discontinuous growth process mainly came from the pinning pressure generated by nanoscale precipitates.

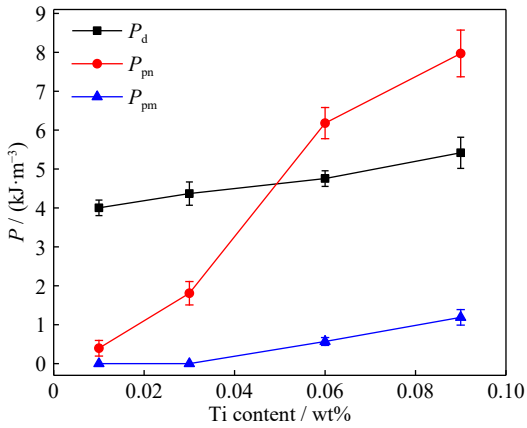

Fig. 14. Driving pressure and pinning pressure for CCG growth.

The higher value of P_{pm} in the 0.09Ti sample is mainly since the number of precipitates is much greater than in the 0.06Ti sample for micron-scale particles, although the precipitate size was lightly smaller. That is, when the precipitate size was smaller and the number of precipitates was greater, the pinning force was greater. This theory also applies to nanoscale precipitates. Therefore, the inhibition of discontinuous growth can be maximized by optimizing the technical parameters, such as the cooling rate, to change the distribution of Ti(C,N) particles at a particular titanium content, which remains a topic for future work.

4. Conclusions

The influence of titanium addition on the refinement of CCGs in peritectic carbon steel was studied with a fast-directional solidification experiments that can produce γ grain structure similar to that from a practical continuous casting process. The important points in the present study are summarized as follows.

(1) The addition of titanium not only decreased the CCG region but also decreased the short-axis diameters of the CCG structures. When the addition of titanium was 0.09wt%, the CCG structure was completely suppressed.

(2) The nanoscale Ti(C,N) would precipitate with the decrease of transition temperature from FCG to CCG and the size of nanoscale Ti(C,N) increase from 2.4 to 30.2 nm, meanwhile, the volume fraction increase from 0.0007% to 0.023% with the increase of Ti from 0.01wt% to 0.09wt% at FCRB after solidification of 30 s.

(3) The pinning pressure provided by microscale and nanoscale Ti(C,N) was 7.75 kJ·m^{-3}, which was greater than the driving pressure of 4.75 kJ·m^{-3} at FCRB in 0.06Ti sample, and the migration of the FCG/CCG boundary was suppressed at this position, which indicated the refinement of CCG was ascribed to the Ti(C,N) particles.

Acknowledgements

The present work is financially supported by the National Natural Science Foundation of China (Nos. 51774075 and 52174307), Liao Ning Revitalization Talents Program, China (No. XLYC1802032). The authors greatly appreciate their support.

Conflict of Interest

The authors declare no conflict of interest.

References

[1] M. Ohno, S. Tsuchiya, and K. Matsuura, Microstructural features and formation processes of as-cast austenite grain structures in hypoperitectic carbon steels, *ISIJ Int.*, 55(2015), No. 11, p. 2374.

[2] H. T. Tasi, H. Yin, M. Lowry and S. Morales, Analysis of transverse corner cracks on slabs and countermeasures, *Iron Steel Technol.*, 3(2006), p. 23.

[3] B. Mintz and J.M. Arrowsmith, Hot-ductility behaviour of C–Mn–Nb–Al steels and its relationship to crack propagation during the straightening of continuously cast strand, *Met. Technol.*, 6(1979), No. 1, p. 24.

[4] H. Yasuda, T. Suga, K. Ichida, T. Narumi, and K. Morishita, *In situ* observation of austenite coarsening induced by massive-like transformation during solidification in Fe–C alloys, *IOP Conf. Ser.: Mater. Sci. Eng.*, 861(2020), No. 1, art. No. 012051.

[5] G. Azizi, B.G. Thomas, and M. Asle Zaeem, Review of peritectic solidification mechanisms and effects in steel casting, *Metall. Mater. Trans. B*, 51(2020), No. 5, p. 1875.

[6] N.S. POttore, C.I. Garcia, and A.J. DeArdo, Interrupted and isothermal solidification studies of low and medium carbon steels, *Metall. Trans. A*, 22(1991), No. 8, p. 1871.

[7] T. Maruyama, K. Matsuura, M. Kudoh, and Y. Itoh, Peritectic transformation and austenite grain formation for hyper-peritectic carbon steel, *Tetsu-to-Hagane*, 85(1999), No. 8, p. 585.

[8] N. Yoshida, O. Umezawa, and K. Nagai, Analysis on refinement of columnar γ grain by phosphorus in continuously cast 0.1 mass% carbon steel, *ISIJ Int.*, 44(2004), No. 3, p. 547.

[9] S. Tsuchiya, M. Ohno, K. Matsuura, and K. Isobe, Formation mechanism of coarse columnar γ grains in as-cast hyperperitectic carbon steels, *Acta Mater.*, 59(2011), No. 9, p. 3334.

[10] M. Ohno, S. Tsuchiya, and K. Matsuura, Formation conditions of coarse columnar austenite grain structure in peritectic carbon steels by the discontinuous grain growth mechanism, *Acta Mater.*, 59(2011), No. 14, p. 5700.

[11] S. Kencana, M. Ohno, K. Matsuura, and K. Isobe, Effects of Al and P additions on as-cast austenite grain structure in 0.2 mass% carbon steel, *ISIJ Int.*, 50(2010), No. 12, p. 1965.

[12] S. Tsuchiya, M. Ohno, K. Matsuura, and K. Isobe, Effects of Cr addition on coarse columnar austenite structure in as-cast 0.2 mass% carbon steel, *ISIJ Int.*, 50(2010), No. 12, p. 1959.
[13] Y.L. Wang, Y.L. Chen, and W. Yu, Effect of Cr/Mn segregation on pearlite–martensite banded structure of high carbon bearing steel, *Int. J. Miner. Metall. Mater.*, 28(2021), No. 4, p. 665.
[14] S.F. Medina, M. Chapa, P. Valles, A. Quispe, and M.I. Vega, Influence of Ti and N contents on austenite grain control and precipitate size in structural steels, *ISIJ Int.*, 39(1999), No. 9, p. 930.
[15] X.L. Wan, K.M. Wu, G. Huang, R. Wei, and L. Cheng, *In situ* observation of austenite grain growth behavior in the simulated coarse-grained heat-affected zone of Ti-microalloyed steels, *Int. J. Miner. Metall. Mater.*, 21(2014), No. 9, p. 878.
[16] B. Feng, T. Chandra, and D.P. Dunne, Effect of alloy nitride particle size distribution on austenite grain coarsening in Ti and Ti–Nb bearing HSLA steels, *Mater. Forum*, 13(1989), No. 2, p. 139.
[17] R. Vaz Penna, L.N. Bartlett, and R. O'Malley, Influence of TiN additions on the microstructure of a lightweight Fe–Mn–Al steel, *Int. J. Metalcast.*, 14(2020), No. 2, p. 342.
[18] A. Graux, S. Cazottes, D. de Castro, D. San Martín, C. Capdevila, J.M. Cabrera, S. Molas, S. Schreiber, D. Mirković, F. Danoix, M. Bugnet, D. Fabrègue, and M. Perez, Precipitation and grain growth modelling in Ti–Nb microalloyed steels, *Materialia*, 5(2019), art. No. 100233.
[19] R. Wei, C.J. Shang, and K.M. Wu, Grain refinement in the coarse-grained region of the heat-affected zone in low-carbon high-strength microalloyed steels, *Int. J. Miner. Metall. Mater.*, 17(2010), No. 6, p. 737.
[20] M. Ohno and K. Matsuura, Refinement of as-cast austenite microstructure in S45C steel by titanium addition, *ISIJ Int.*, 48(2008), No. 10, p. 1373.
[21] S. Tsuchiya, M. Ohno, and K. Matsuura, Transition of solidification mode and the as-cast γ grain structure in hyperperitectic carbon steels, *Acta Mater.*, 60(2012), No. 6-7, p. 2927.
[22] Y. Maehara, K. Yasumoto, Y. Sugitani, and K. Gunji, Effect of carbon on hot ductility of as-cast low alloy steels, *ISIJ Int.*, 25(1985), No. 10, p. 1045.
[23] L.T. Gui, M.J. Long, H.H. Zhang, D.F. Chen, S. Liu, Q.Z. Wang, and H.M. Duan, Study on the precipitation and coarsening of TiN inclusions in Ti-microalloyed steel by a modified coupling model, *J. Mater. Res. Technol.*, 9(2020), No. 3, p. 5499.
[24] Y. Huang, W.N. Liu, A.M. Zhao, J.K. Han, Z.G. Wang, and H.X. Yin, Effect of Mo content on the thermal stability of Ti–Mo-bearing ferritic steel, *Int. J. Miner. Metall. Mater.*, 28(2021), No. 3, p. 412.
[25] T. Kato, Y. Ito, M. Kawamoto, A. Yamanaka, and T. Watanabe, Prevention of slab surface transverse cracking by microstructure control, *ISIJ Int.*, 43(2003), No. 11, p. 1742.
[26] I. Andersen and Ø. Grong, Analytical modelling of grain growth in metals and alloys in the presence of growing and dissolving precipitates—I. Normal grain growth, *Acta Metall. Mater.*, 43(1995), No. 7, p. 2673.
[27] G.E. Pellissier and S.M. Purdy, *Stereology and Quantitative Metallography*, American Society for Testing and Materals, Easton, 1972.